

HLA Implementation of the TITAN Optics System

Meagan Stewart

University of Waterloo

Abstract: The purpose of this report is to detail the creation of the TITAN beam envelope model through the transport beam line and to their measurement Penning trap, as well as to determine the accuracy of this model by taking measurements of the beam. Positions of the elements in the beam line were taken from mechanical drawings provided by the TRIUMF design office and added to the High Level Application (HLA) database, allowing TRANSOPTR to be run to simulate the beam envelope through the transport line to MPET. The Einzel lenses along the beam path were modelled using *Opera2D* to find their potential map, as the TITAN Einzel lens geometries differ from the native TRANSOPTR implementation. Tests were performed using the TITAN beam line at diagnostic elements ILE2T:RPM3 and TRFCBL:MCP1 at 12keV, 15keV, and 20keV beam energies.

Contents

Abbreviations	2
1 Introduction	3
2 HLA Implementation	4
3 TITAN Experiment Source Material	4
3.1 MPET	4
3.2 MRTOF	11
4 Opera2D Modelling	12
5 TRANSOPTR Simulations	19
6 TITAN Beam Measurements	22
6.1 ILE2T:RPM3	22
6.2 TRFCBL:MCP1	28
7 Conclusion	32
References	33

Abbreviations

AXEZ: Axial electric field (TRANSOPTR subroutine)

DEFL: Deflector

EB: Electrostatic bender

ECB: Electrostatic correction bender (Steering plates)

EL: Einzel lens

EQ: Electrostatic quadrupole

FC: Faraday cup

HLA: High Level Applications

IV: Isolation valve

MCP: Micro-channel plate

MPET: Measurement Penning trap

MRTOF: Multi-reflection time of flight

RFQ: Radio frequency quadrupole

RPM: Rotary profile monitor

SK: Skimmer plate

TIS: TITAN ion source

TITAN: TRIUMF's ion trap atomic nuclear science

1 Introduction

The TITAN experiment at TRIUMF is designed to perform precise mass measurements using ion trapping techniques. Its main transport beam line links a radio frequency quadrupole (RFQ) cooler-buncher [1] travelling into a measurement Penning trap (MPET), spanning approximately seven metres. RFQ extracted beam can also travel through a series of Einzel lenses to the multi-reflection time of flight (MRTOF) spectrometer for time-of-flight mass filtration. Within both possible beam line trajectories there are multiple optical elements that are used to focus and match the beam, as these experimental devices require a well-matched beam to perform high-precision mass measurements.

The beam physics team was asked to provide a model for both the MPET and MRTOF beam line trajectories and integrate it into the High Level Applications (HLA) [2] for a more convenient way of tuning. Element positions along the beam line, in addition to characteristic dimensions such as lengths and apertures were obtained via mechanical drawings provided by the experiment. these were then uploaded to the HLA database (sometimes referred to as the `/acc` database), stored in `xml` format. From these files, a Python script is then run to convert the code into a Fortran document which can then be run with `TRANSOPTR`—a linear optics code which computes the evolution of the second moments of the beam distribution, including space charge, and then outputs the modelled beam envelope [3]. Using this envelope, one is able to adjust the settings of the elements to change the location of tight focuses and provide optimal tunes at the locations of diagnostic elements as well as the eventual ion traps.

For Einzel lenses, the `TRANSOPTR` subroutine assumes a specific lens geometry which differs from the TITAN lenses [4]. In order to model the beam envelope through the beam line, the electric field through each of these lenses was recreated using the electromagnetic simulation software `Opera2D` [5] by taking advantage of the cylindrical symmetry of the beam pipe. The field maps generated were then added to the `xml` database and integrated into the `TRANSOPTR` implementation to calculate the envelope through TITAN's transport optics. In order to test this implementation, the TITAN offline ion source (TIS) was used to fly beam through the MPET beam line and compare the behaviour of the beam to the individual `Opera` models as well as the `TRANSOPTR` model as a whole.

This note will include details of the design drawing measurements and addition of the optical elements into the `xml` database (including the current state of available beam diagnostics), the `Opera` modelling of the Einzel lenses, and the future implementation of HLA for more convenient beam tuning and analysis for TITAN. It will also discuss the results of the tests conducted using the TIS to determine the validity of the TITAN implementation, including analysis of data collected with a rotary profile monitor (RPM) before the RFQ and psuedoquantitative analysis of a multi-channel plate (MCP) after the RFQ.

2 HLA Implementation

In the HLA /acc database, sections of beam are divided into sequences. These sequences are pieces of `xml` code that consist of a unique piece of beam line, and consecutively orders the beam line elements in relation to each other. Each element is given an `xml` tag in the sequence where its optical and physical properties are defined. The sequences are then stacked to create discrete beam paths, used along side a tune file to eventually run TRANSOPTR. This HLA tune file provides the initial conditions of the beam as well as the element set points for beam transport. Within each element tag in the sequence, the optical properties are listed, as well as referencing the element's tag in the tune file to link the element attribute to the tune value.

Using the `xml` path and tune files in the database, a Python script is called to convert the path into a Fortran `sy.f` file and a `data.dat` file. The `sy.f` file contains Fortran subroutines called for each type of element using the attributes in the sequence files, and the `data.dat` file contains the element values and initial beam conditions as entered in the tune file. These files are then run with TRANSOPTR, which computes the theoretical beam envelope.

3 TITAN Experiment Source Material

3.1 MPET

The beam line from the TIS to MPET in the /acc database is a path titled `tis-mpet.xml` and contains sequences `tis1_db0.xml`, `tis1_db1.xml`, `ile2t_db3.xml`, `trfc_db1.xml`, `trfc_db5.xml`, `trfcbl_db1.xml`, `tsybl_db0.xml`, and `mpetbl_db1.xml`. Positions and dimensions of the elements in each sequence were verified using drawings provided either by the TRIUMF Design Office or by the experiment team themselves. DraftSight [6] software was used to obtain measurements from the drawings in inches, which was then converted to millimetres using a conversion factor of 25.4 mm per inch. The starting coordinates of each sequence provided in later tables are in reference to the drawing listed in Table 1.

Sequence	ref. DWG(s)	Figure	Table
<code>tis1_db0.xml</code>	IEX0402D-revA01	Figure 1	Table 2
<code>tis1_db1.xml</code>	IEX0402D-revA01 and IEX0403D-revA	Figure 1 and 2	Table 3
<code>ile2t_db3.xml</code>	ISK4369D-revG	Figure 3	Table 4
<code>trfc_db1.xml</code>	ISK4369D-revG	Figure 3	Table 5
<code>trfc_db5.xml</code>	ISK4369D-revG	Figure 3	Table 6
<code>trfcbl_db1.xml</code>	ISK4369D-revG	Figure 3	Table 7
<code>tsybl_db0.xml</code>	IEX0695D-revA and ISK4457D-rev3	Figure 4 and 5	Table 8
<code>mpetbl_db1.xml</code>	IEX0695D-revA	Figure 4	Table 9

Table 1: List of sequences in path and the design drawings used for their construction.

Sequence tis1-db0			
Start (x,y)		End (x,y)	
(9.886", 12.495")		(9.886", 17.758")	
Element Name	Element Type	Position S(mm)	Length L(mm)
TIS1:XCB0	ECB	76.987	19.050
TIS1:YCB0	ECB	106.197	19.050
Total: 133.680 mm			

Table 2: Sequence tis1-db0, beginning at anode of ion source and terminating at end of aperture before ILE cross section.

A note should be made for the next sequence (`tis1_db1.xml`), as there is no drawing that includes both the aperture after steerers TIS1:XCB0 and TIS1:YCB0 and the aperture before the TIS Einzel lens TIS1:EL1. Therefore, the distance was given to us by the experiment team to be 286.440 mm, from the top of the last aperture of Figure 1 to the bottom of the first aperture on Figure 2. `tis1_db1.xml` also ends on a deflector that is not present in drawing IEK0403D, and the distance from the end of the TIS section to the deflector which begins the next sequence was also provided as 579.471 mm. Apertures are not included in the HLA framework unless they contribute to the optics (i.e. are not grounded).

It should also be noted that the lengths of any Einzel lenses are not the lengths of the devices themselves, but the field that they create. This will be discussed more in depth in the Opera2D modelling section.

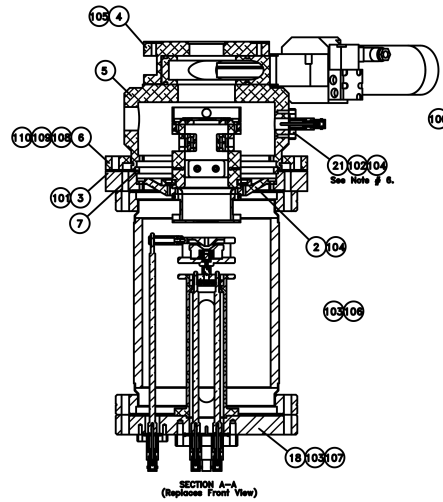


Figure 1: IEX0402: TIS Anode and beginning of ILE cross section.

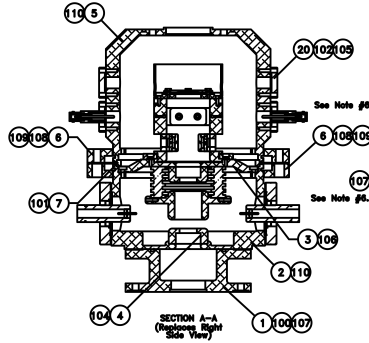


Figure 2: IEX0403: TIS steerers and Einzel lens.

Sequence tis1-db1			
Start (IEX0402D) (x,y)		End (ISK4369D) (x,y)	
(9.886", 17.758")		(0.02888", 27.92116")	
Start ref. aperture (IEX0403D) (x,y)		End ref. aperture (IEX0403D) (x,y)	
(31.648", 6.241")		(31.648", 15.988")	
Element Name	Element Type	Position S(mm)	Length L(mm)
TIS1:EL1	EL	335.310	244.805
TIS1:XCB1	ECB	405.337	19.050
TIS1:YCB1	ECB	434.547	19.050
ILE2T:YCB3	ECB	1036.726	50.800
Total from TIS: 1170.406 mm			

Table 3: Sequence tis1-db1, beginning at end of aperture before ILE cross section and terminating end of at steerer ILE2T:YCB3. The reference apertures are the reference points from which all elements on the drawing are measured, with the distance between them being 286.440 mm as provided by the TITAN experimental team.

Sequence ile2t-db3			
Start (x,y)		End (x,y)	
(0.02888", 27.92116")		(-0.0124", 37.53216")	
Element Name	Element Type	Position S(mm)	Length L(mm)
ILE2T:RPM3	RPM	42.941	0.00
ILE2T:FC3	FC	93.487	0.00
ILE2T:XCB3	ECB	150.419	0.00
ILE2T:Q3	EQ	220.281	61.468
Total from TIS: 2781.093 mm			

Table 4: Sequence ile2t-db3, beginning at end of steerer ILE2T:YCB3 and terminating at end of quadrupole ILE2T:Q3.

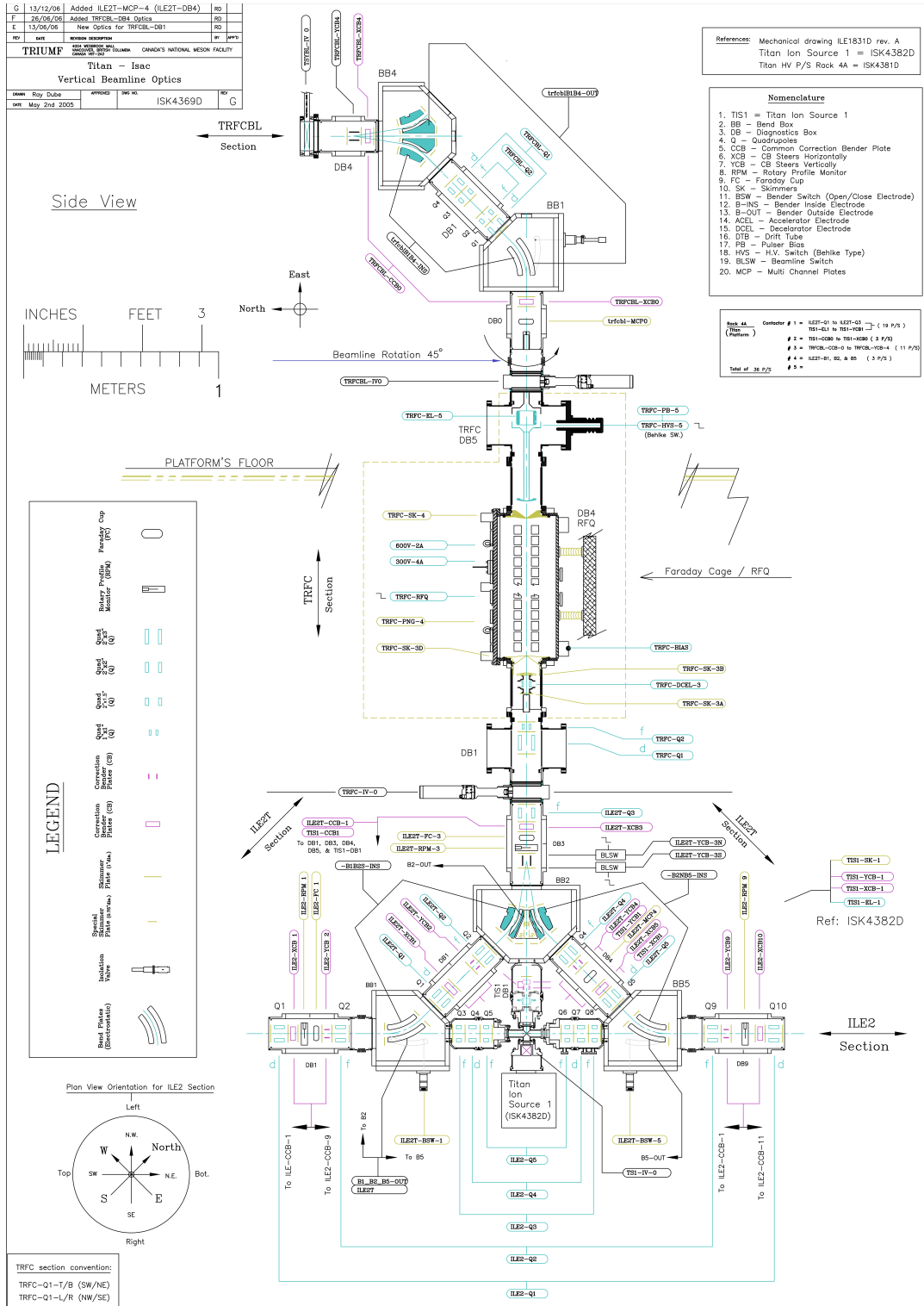


Figure 3: ISK4369D: TITAN vertical beam line optics.

Sequence trfc-db1			
Start (x,y)		End (x,y)	
(-0.01242", 37.53216")		(-0.01242", 64.81948")	
Element Name	Element Type	Position S(mm)	Length L(mm)
TRFC:IV0	IV	81.945	0.00
TRFC:Q1	EQ	335.185	86.868
TRFC:Q2	EQ	418.303	30.734
TRFC:DCEL3	AXEZ	633.693	100.000
Total from TIS: 3473.421 mm			

Table 5: Sequence trfc-db1, beginning at end of quadrupole ILE2T:Q3 and terminating on skimmer TRFC:SK3B after decelerator.

The sequence contained in Table 6 includes the RFQ cooler-buncher. However, we have no way of modelling buffer gas cooling in TRANSOPTR so it is included in HLA as a marker (just a label to denote its position, written as element type MARK). While the sequence actually starts at the skimmer after TRFC:DCEL3 when keeping with HLA naming/sequencing convention, all simulations are run from TRFC:SK4 which is the first skimmer after the RFQ. This can be done as the cooling and bunching which takes place in the RFQ changes the emittance of the beam. Output RFQ beam may be considered as a new set of initial conditions for subsequent TRANSOPTR simulations starting at the skimmer. The position of this skimmer will also be included as a marker. It should be noted that all elements in this sequence when run in TRANSOPTR will have a position offset of 793.171mm, as that is the distance from the start of the sequence (TRFC:SK3B before the RFQ) to TRFC:SK4.

Sequence trfc-db5			
Start (x,y)		End (x,y)	
(-0.01242", 64.81948")		(-0.01242", 121.48306")	
Element Name	Element Type	Position S(mm)	Length L(mm)
TRFC:RFQ	MARK	441.692	704.821
TRFC:SK4	MARK	793.171	0.00
TRFC:EL5	EL	1308.135	263.550
Total from TIS: 4912.044 mm			
Total from SK4: 645.452 mm			

Table 6: Sequence trfc-db5, beginning on skimmer TRFC:SK3B after decelerator and terminating at end of faraday cage enclosing RFQ and Einzel lens.

Sequence trfcbl-db1			
Start (x,y)		End (x,y)	
(-0.01342", 121.48306")		(-35.78747", 173.13889")	
Element Name	Element Type	Position S(mm)	Length L(mm)
TRFCBL:IV0	IV	53.828	60.230
TRFCBL:MCP0	MCP	362.496	25.400
TRFCBL:EL0	EL	435.033	149.215
TRFCBL:B1	EB	688.981	199.491
TRFCBL:Q1	EQ	905.541	49.022
TRFCBL:Q2	EQ	975.391	36.322
TRFCBL:MCP1	MCP	1049.293	0.00
TRFCBL:Q3	EQ	1123.194	36.322
TRFCBL:Q4	EQ	1193.044	49.022
TRFCBL:B4	EB	1483.838	159.593
TRFCBL:XCB4	ECB	1731.496	25.400
TRFCBL:XYCB4	DEFL	1804.909	50.4
Total from TIS: 6740.753 mm			
Total from SK4: 2474.161 mm			

Table 7: Sequence trfcbl-db1, beginning at end of faraday cage enclosing RFQ and Einzel lens and terminating at end of deflector TRFCBL:YCB4.

Sequence tsybl-db0			
Start (IEX0695D) (x,y)		End (IEX0695D) (x,y)	
(274.711", 132.301")		(169.912", 132.302")	
Element Name	Element Type	Position S(mm)	Length L(mm)
TSYBL:IV0	IV	18.365	19.558
TSYBL:XCB0	ECB	475.463	25.400
TSYBL:EL1	EL	868.299	309.880
TSYBL:EL3	EL	1913.788	309.880
TSYBL:XCB8	ECB	2306.472	25.400
TSYBL:EL4	EL	2636.495	318.059
Total from TIS: 9402.648 mm			
Total from SK4: 5136.056 mm			

Table 8: Sequence tsybl-db0, beginning at end of deflector TRFCBL:YCB4 and terminating at end of TSYBL:EL4. Note that the positions of the steerers were found by measuring backwards on drawing ISK4457D from Einzel lenses as they are not on IEX0695D.

Sequence mpetbl-db1			
Start (x,y)		End (x,y)	
(169.912", 132.302")		(88.960", 132.302")	
Element Name	Element Type	Position S(mm)	Length L(mm)
MPETBL:IV0	IV	345.973	0.00
MPETBL:EL2	EL	1077.773	378.460
MPETBL:XCB3	ECB	1593.621	25.400
MPETBL:XCB3	ECB	1631.772	25.400
Total from TIS: 11662.030 mm			
Total from SK4: 7395.438 mm			

Table 9: Sequence mpetbl-db1, beginning at end of TSYBL:EL4 and terminating on unlabelled diagnostic tool that sits on last stand before MPET chamber.

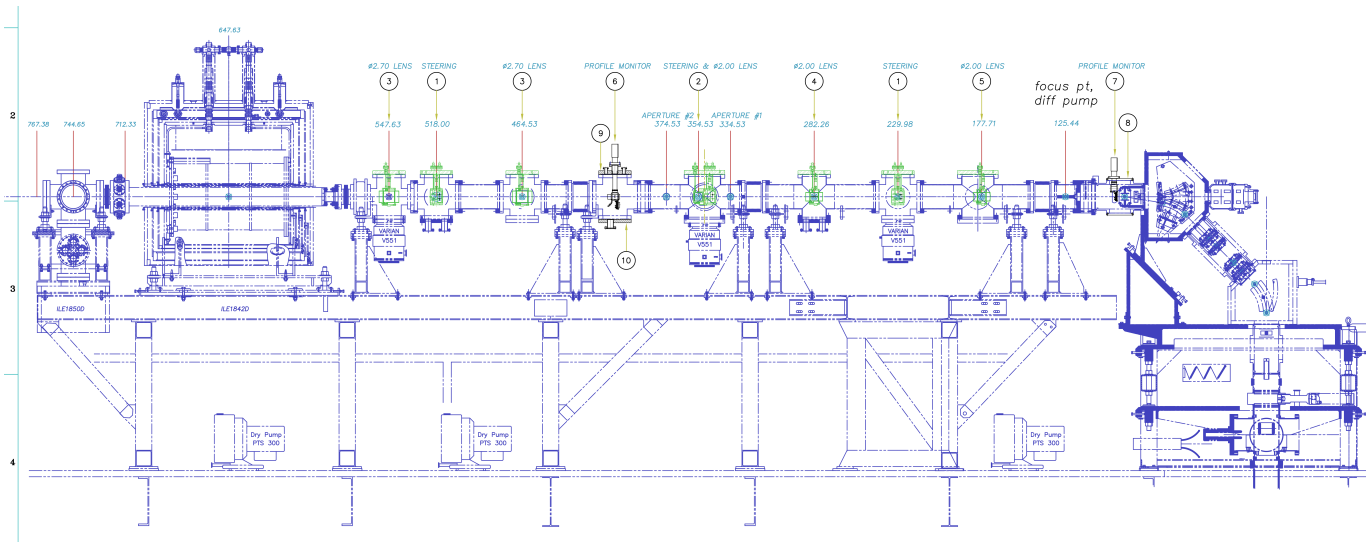


Figure 4: IEX0695D: TITAN Penning trap optics layout.

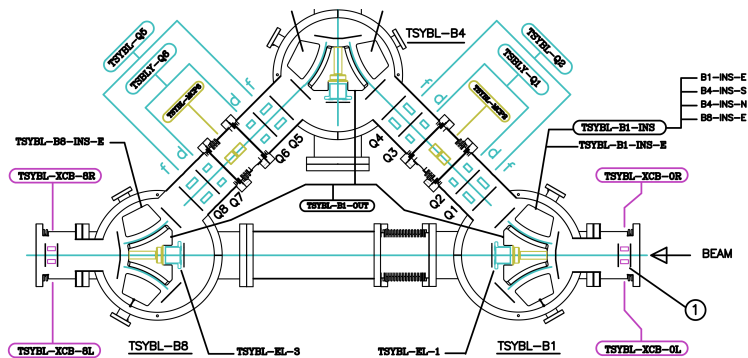


Figure 5: ISK4457D: TITAN EBIT bender section.

3.2 MRTOF

The beam line from the TIS to MPET in the /acc database is a path titled `trfc-mrtof.xml` and contains sequences `trfc_db5.xml`, `trfcbl_db0.xml`, and `mrtofbl_db1.xml`. This path has omitted the earlier TIS and ILE2T sequences, as the RFQ effectively changes the initial beam conditions for the remainder of the TITAN optics and unless testing the TIS, TRANSOPTR is always run from TRFC:SK4 in `trfc_db5.xml`. While the beam may initially start at the TIS, the initial sequences can be omitted. The sequence `trfc_db5.xml` remains unchanged in this path, and has already been detailed in Table 6 so will not be repeated. The sequence `mrtofbl_db1.xml` is entirely modelled in Opera2D, and will be discussed later in this note. The sequence `trfcbl_db0.xml` is identical to `trfcbl_db1.xml`, except it stops after TRFCBL:EL0 and undergoes a long drift with no elements straight through the bender to the MRTOF section (see 519.4mm drift as shown in Figure 6). The optical elements in the sequence have the same positions and dimensions as those in `trfcbl_db1.xml`.

No detailed mechanical or technical drawings of the MRTOF beam line were found to provide dimensions, however images were supplied by the experiment team that details the positions of the elements from the bender section to the beginning of MRTOF (Figures 6 and 7).

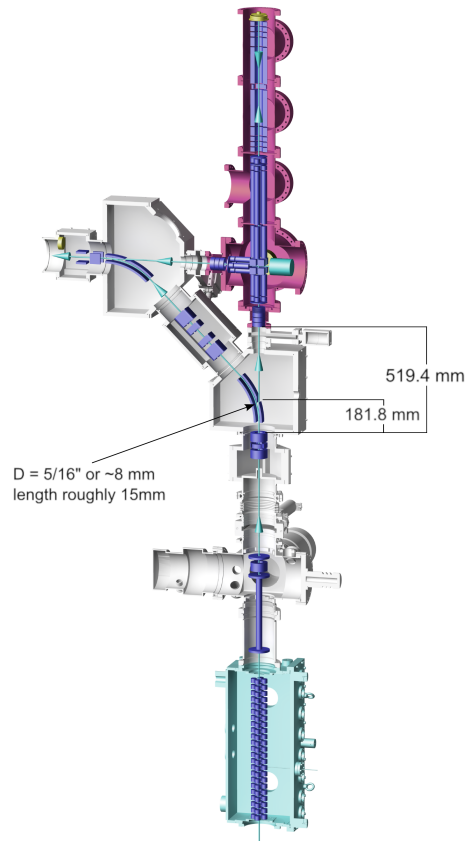


Figure 6: MRTOF beam line positions and distances as provided by TITAN experiment team.

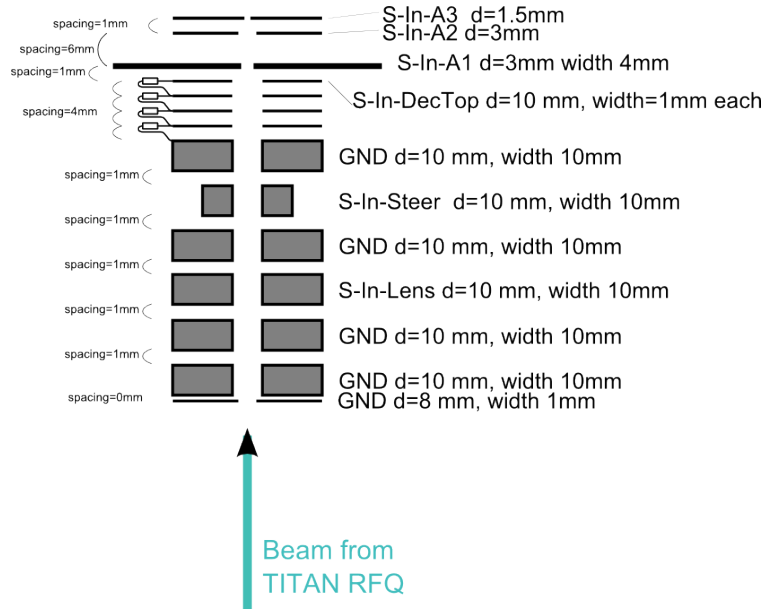


Figure 7: MRTOF input optics as provided by TITAN experiment team. Note that "GND" means the element is grounded, whereas "S-In-Lens", "S-In-Steer", etc. means the element has applied voltage.

4 Opera2D Modelling

As seen in the previous section, the TITAN transport beam line is comprised of multiple Einzel lenses, specifically in the areas between the 90°bender after the RFQ and MPET shown in Figure 4, and the area before MRTOF shown in Figure 7. While TRANSOPTR has a callable Einzel lens subroutine, the geometry of the lens it simulated was not consistent with the lenses present in the TITAN beam line with the TRANSOPTR subroutine lens assuming fixed proportions not corresponding to the TITAN lenses. Even within the same beam line, the geometry of the sequential lenses differed greatly, as they were custom developed by the experiment to satisfy their different constraints. TRANSOPTR does however have a subroutine for integrating and scaling one dimensional potential maps externally so long as the electric fields are axially symmetric. Taking advantage of the cylindrical symmetry of the lenses, each Einzel lens in the TITAN transport beam line was modelled using the code Opera2D allowing for custom potential map production. The dimensions for each lens (tube thickness, edge radii of curvature, length, etc.) were provided either by the TITAN experiment team or found using mechanical drawings shown in Figures 2 and Figures 8 (a), (b), and (c).

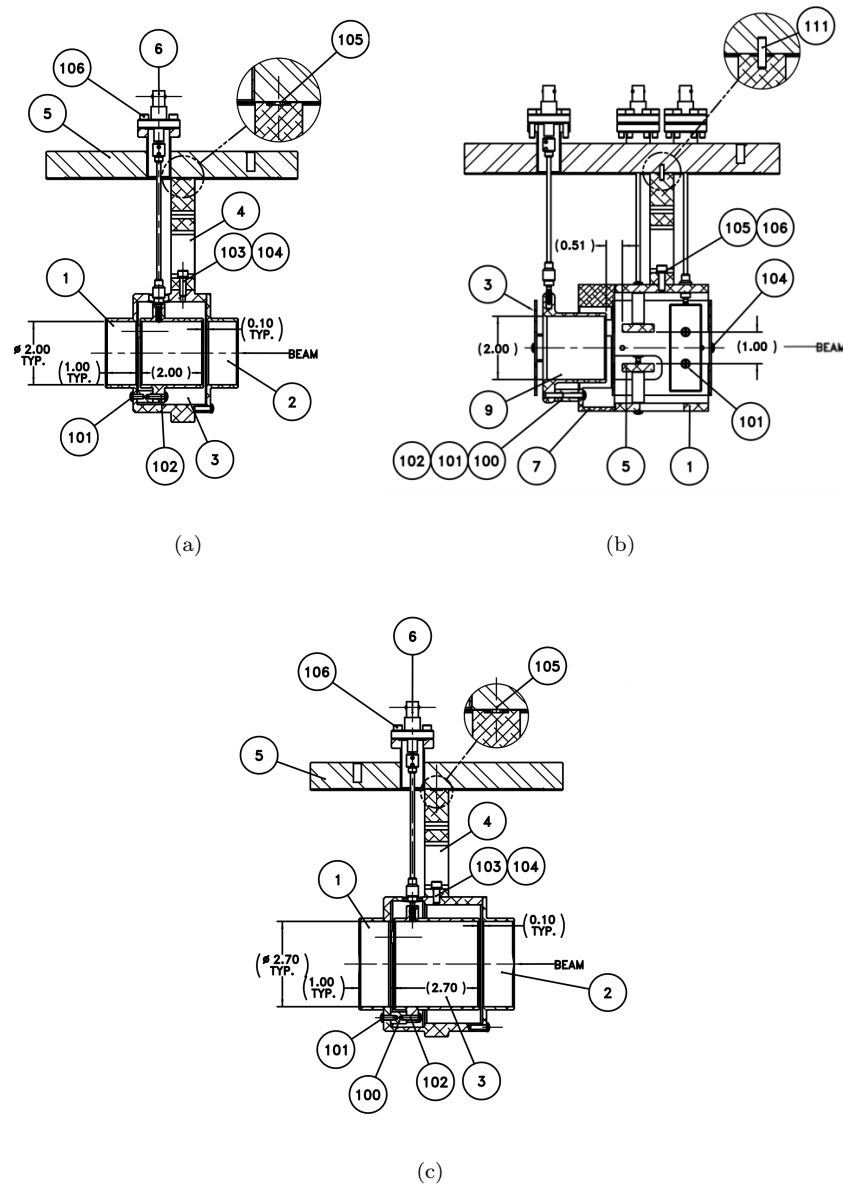


Figure 8: (a) 2" Einzel lens assembly for TSYBL:EL1 and TSYBL:EL3. (b) Steering and 2" Einzel lens assembly for TSYBL:EL4. (c) Einzel lens assembly for MPETBL:EL2.

Figure 9 is an example of an Opera2D model created for TRFCBL:EL0, one of the less complex geometries in the transport beam line. Note that the beam pipe on the far right, as well as the first and last lens tubes are grounded, whereas the middle tube is set to 1kV. All elements in these Opera2D models that are not grounded are biased at either 1kV or -1kV, the resulting potential mapping is then normalized providing an easily scalable potential for lens simulation.

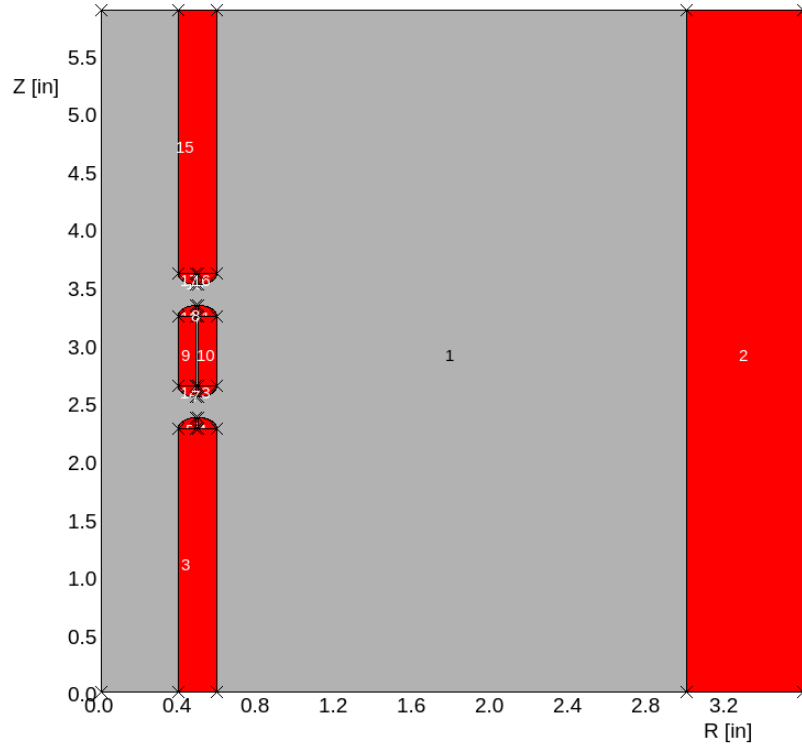


Figure 9: Opera2D Model of TRFCBL:EL0 from information provided by TITAN experiment team. Note in this figure that the beam propagation direction runs from the bottom of the figure to the top, with the optical axis of the device defined vertically at $R=0.0$ inches.

The Einzel lens name, lens dimension source drawing, and the figure number of the potential map are all listed in Table 10. Dimensions provided by the TITAN team, such as the radius of curvature of the rounded edges in Figure 9 for example, were taken directly from TITAN experiment models of the lenses as there were no design drawings available from the TRIUMF design office.

Einzel Lens	Dimensions provider	Potential Map
TIS:EL1	IEX0403D-revA (Figure 2)	Figure 10
TRFC:EL5	TITAN experiment team	Figure 11
TRFCBL:EL0	TITAN experiment team	Figure 12
TSYBL:EL1	IEX0724C-revA (Figure 8a)	Figure 13
TSYBL:EL3	IEX0724C-revA (Figure 8a)	Figure 13
TSYBL:EL4	IEX0696C-revA (Figure 8b)	Figure 14
MPETBL:EL2	IEX0717C-revA (Figure 8c)	Figure 13

Table 10: List of Einzel lenses, source material, and the figure number of their potential map.

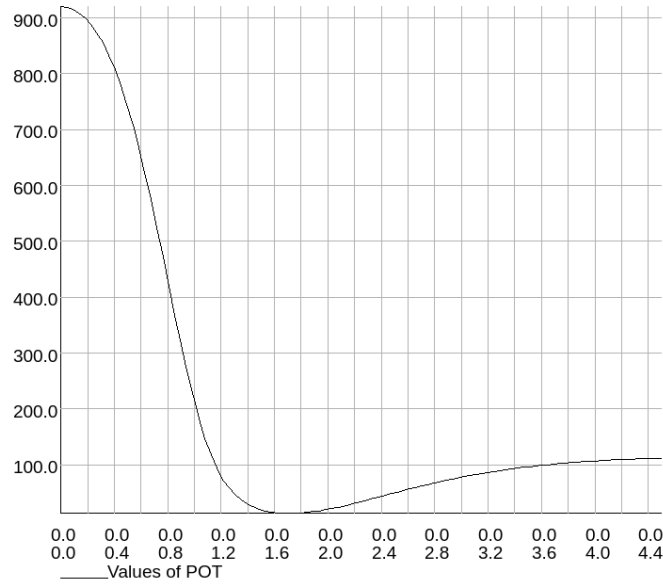


Figure 10: Potential map generated from the Opera2D model of TIS:EL1 with dimensions from IEX0303D. The X axis shows the beam path in inches, and the Y axis shows the potential in volts.

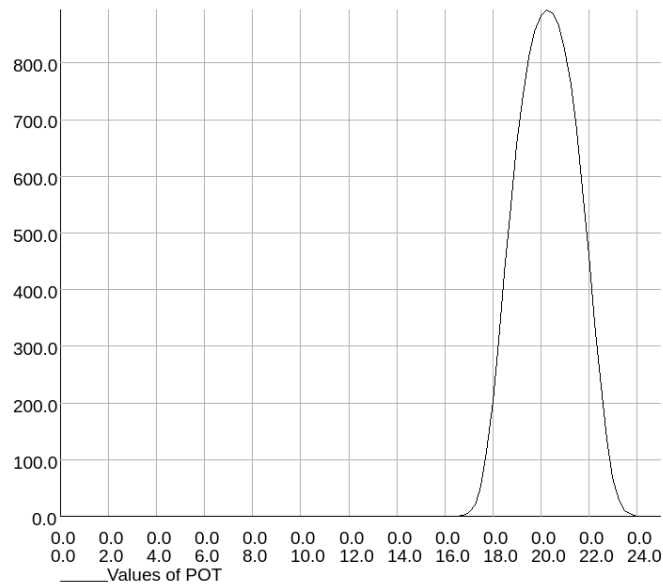


Figure 11: Potential map generated from the Opera2D model of TRFC:EL5 with dimensions from the TITAN experiment team. The X axis shows the beam path in inches, and the Y axis shows the potential in volts.

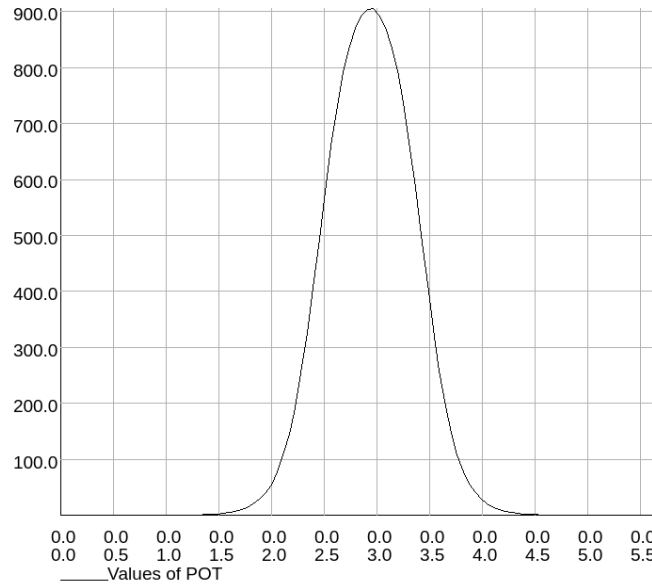


Figure 12: Potential map generated from the Opera2D model of TRFCBL:EL0 with dimensions from the TITAN experiment team. The X axis shows the beam path in inches, and the Y axis shows the potential in volts.

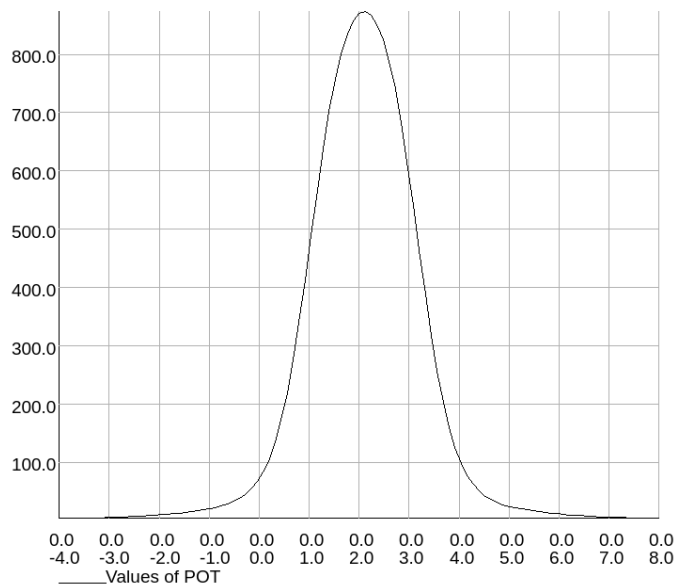


Figure 13: Potential map generated from the Opera2D model of TSYBL:EL1 and TSYBL:EL3 with dimensions from IEX0724C. The X axis shows the beam path in inches, and the Y axis shows the potential in volts.

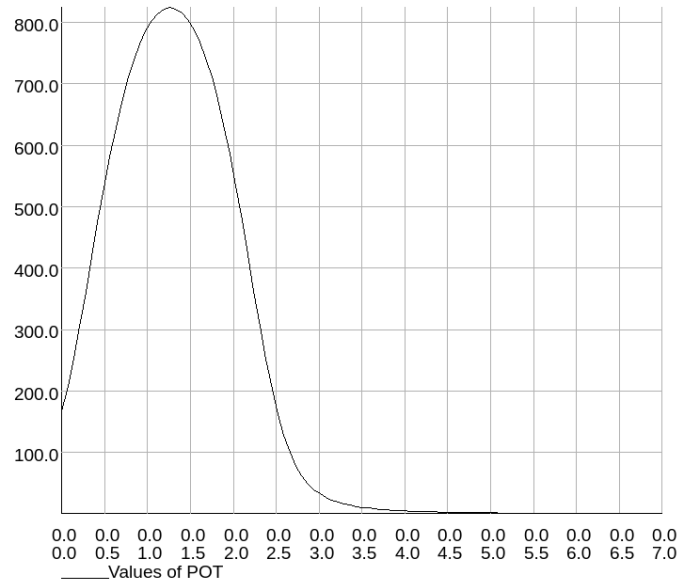


Figure 14: Potential map generated from the Opera2D model of TSYBL:EL4 with dimensions from IEX0696C. The X axis shows the beam path in inches, and the Y axis shows the potential in volts.

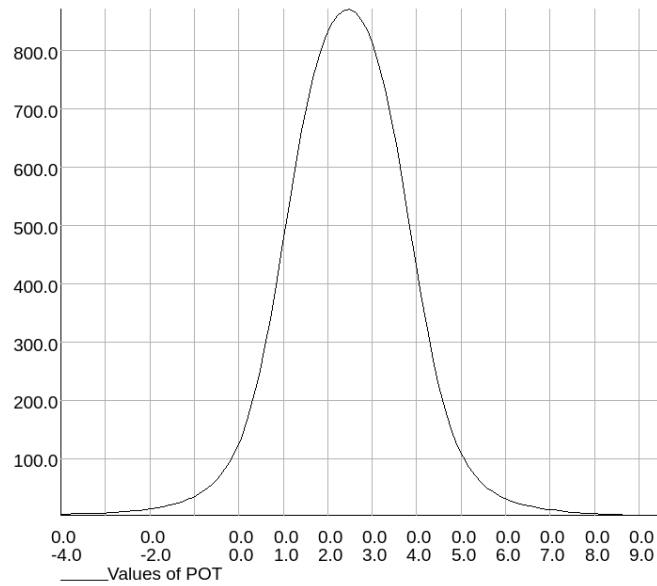


Figure 15: Potential map generated from the Opera2D model of MPETBL:EL2 with dimensions from IEX0717C. The X axis shows the beam path in inches, and the Y axis shows the potential in volts.

Figure 16 is the Opera2D model for the lens stack going into MRTOF that comprises sequence `mrtofb1_db1.xml`. This stack is comprised of an Einzel lens, steerer, decelerator column, and apertures as seen in Figure 7. Note that beam pipe on the far right, as well as the first, second, fourth, and sixth tube counting from the bottom are all grounded. All of the elements in this stack were modelled together as their positions are too close to each other for their electric field contributions to be nonoverlapping. If the experiment wants to run with different bias ratios between adjacent electrodes in the future, more Opera2D field maps will need to be produced.

Table 11 shows the optimal conditions of the MRTOF lens stack as provided by the TITAN experiment team. Due to time constraints, evaluation for different settings on the stack and its effect on the beam envelope have not been conducted. Again, due to the lens stack being modelled in its entirety, at present it is not possible to set values for the individual elements in TRANSOPTR and instead must be scaled as a whole, which implies a preservation of the ratio of element biases. The elements are set to values as shown in Figure 7, for a lens voltage of 1kV.

Element	Optimal Voltage (V)	Normalized Opera2D Voltage (V)
S-In-Lens	-1300	-0.963
S-In-Steer	0	0
S-In-DecTop (plate 1)	281.3	0.208
S-In-DecTop (plate 2)	562.5	0.417
S-In-DecTop (plate 3)	843.8	0.625
S-In-DecTop (plate 4)	1125	0.833
S-in-A1	200	0.148
S-in-A2	1330	0.985
S-in-A3	1350	1.0

Table 11: MRTOF optimal values provided by TITAN experiment team, as well as the normalized Opera2D.

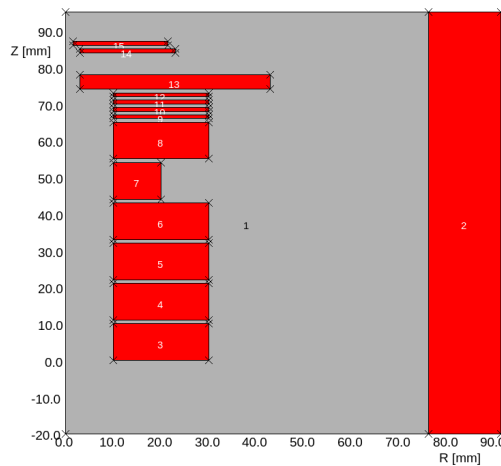


Figure 16: Opera2D Model of lens stack from information provided by TITAN experiment team as shown in Figure 7.

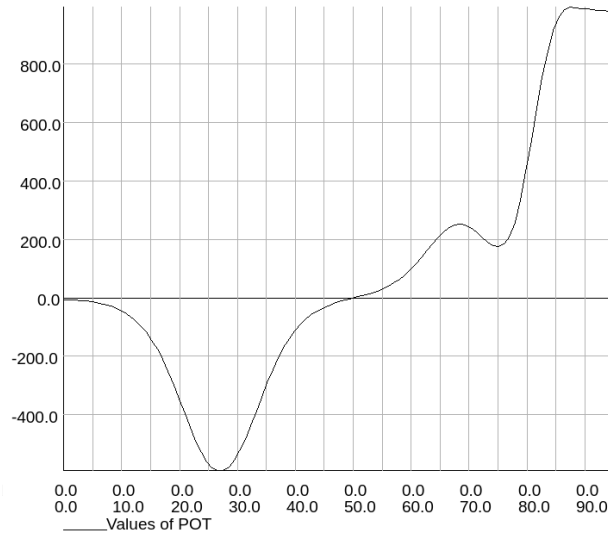


Figure 17: Potential map generated from the Opera2D model of the MRTOF Einzel lens stack. The X axis shows the beam path in millimetres, and the Y axis shows the potential in volts.

5 TRANSOPTR Simulations

Using the Opera models for the Einzel lenses, the TRANSOPTR model was completed with the aforementioned field maps and subroutines for each element. The TRANSOPTR `sy.f` was created from the `/acc` database files using a Python script called `xml2optr`, which converts the specified path and tune of files in the database to `sy.f` and `data.dat` files that can be run with TRANSOPTR. Initial conditions provided by the TITAN experiment team as well as previous beam optics simulations done by the beam physics group. With these, TRANSOPTR envelope calculations were performed at typical TITAN operating beam energies; 2keV and 8keV starting from the RFQ, as well as 20keV starting from the TIS. The TIS TRANSOPTR calculations will be shown in the next section when discussing the measurements performed near the TIS.

To calculate the optimal values for each element to fit the constraints of the beam line (apertures, etc.) a `fit` call was placed in the TRANSOPTR `sy.f` file at the desired location. When run, this allows certain user-specified elements to have their values adjusted to fit the beam envelope through the constraint. Using this feature, and comparing to an example tune provided by the experiment team, optimal element set point values satisfying the fit constraints were calculated along with the envelope. It should be noted that TRFCBL:Q3 and TRFCBL:Q4 have the same power source as TRFCBL:Q1 and TRFCBL:Q2, so while only 2 values will be included in the following tables it is representative of the settings of all four quadrupoles.

Sequence	Sequence Table	Type of Constraint	Radius (cm)	S Position (mm)
tsybl_db0	Table 8	Differential Pumping Aperture (start)	0.4	295.579
tsybl_db0	Table 8	Differential Pumping Aperture (end)	0.4	395.605
tsybl_db0	Table 8	Aperture 1		2436.495
tsybl_db0	Table 8	Aperture 2		2836.493
mpetbl_db1	Table 9	Aperture 1 (end)	0.2	2259.382

Table 12: Locations and radii of fit constraints in sequences, with S positions in reference to the starting coordinates of the drawing located in Table 1 for the corresponding sequence.

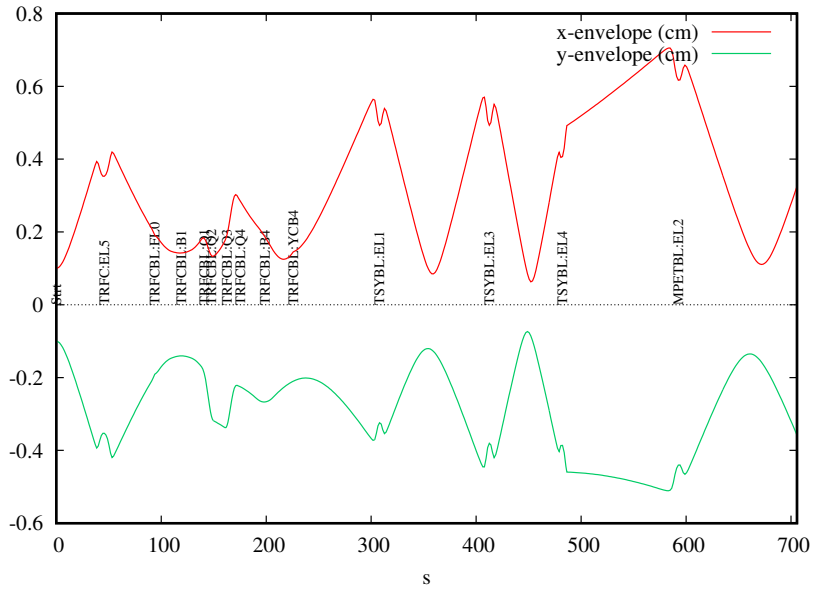


Figure 18: TRANSOPTR envelope simulation for the MPET beam line at 2keV. Element names along the beam line are displayed vertically at the axis.

Element Name	Element Value (V)
TRFC:EL5	-2727
TRFCBL:EL0	-250.0
TRFCBL:Q1	-208.1
TRFCBL:Q2	213.2
TSYBL:EL1	-2212
TSYBL:EL3	-2913
TSYBL:EL4	-1794
MPETBL:EL2	-1718

Table 13: Optimal tune values calculated in TRANSOPTR for each element in the MPET beam line at 2keV, corresponding to the envelope in Figure 18.

mass (MeV)	1.24e+05
x (cm)	0.1
x' (rad)	0.01
y (cm)	0.1
y' (rad)	0.01
z (bunch length, cm)	8.0
dp/p (rad)	0.0018

Table 14: Beam bunch dimensions inputted in TRANSOPTR for the MPET beam line at 2keV, corresponding to the envelope in Figure 18.

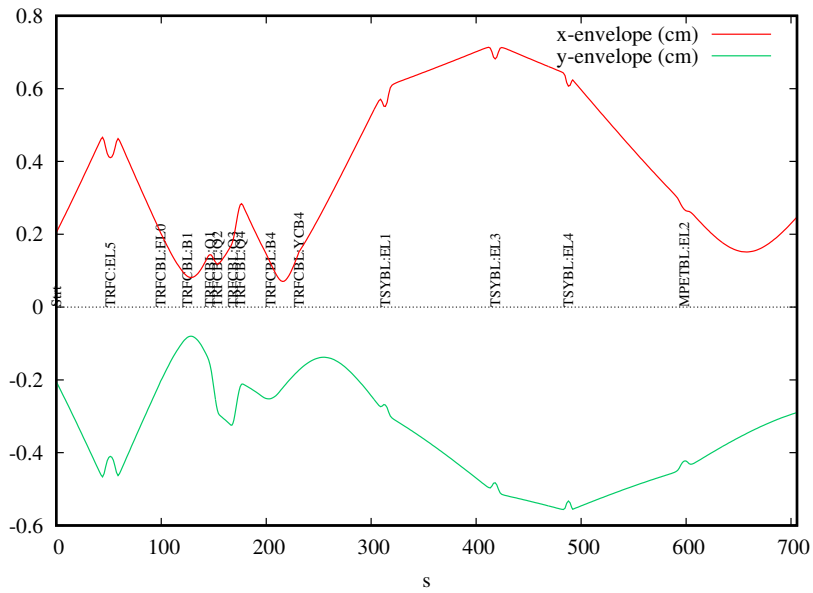


Figure 19: Envelope simulation for the MPET beam line at 8keV. Element names along the beam line are displayed vertically at the axis.

Element Name	Element Value (V)
TRFC:EL5	-8573
TRFCBL:EL0	-250.0
TRFCBL:Q1	-892.7
TRFCBL:Q2	905.6
TSYBL:EL1	-3607
TSYBL:EL3	-2199
TSYBL:EL4	-2000
MPETBL:EL2	-2063

Table 15: Optimal tune values calculated in TRANSOPTR for each element in the MPET beam line at 8keV, corresponding to the envelope in Figure 19.

mass (MeV)	1.24e+05
x (cm)	0.2046
x' (rad)	0.006353
y (cm)	0.2046
y' (rad)	0.006353
z (bunch length, cm)	0.0
dp/p (rad)	1e-05

Table 16: Beam bunch dimensions inputted in TRANSOPTR for the MPET beam line at 2keV, corresponding to the envelope in Figure 18.

6 TITAN Beam Measurements

Measurements using the TIS were performed to test the accuracy of the TRANSOPTR implementation. It should be noted that this is not a test of the accuracy of TRANSOPTR itself, and instead an experiment to determine whether the position values as added to the /acc database are correct as well as the accuracy of the Opera2D Einzel lens models. This experiment could be conducted during TRIUMF winter shutdown due to this TIS being operational and available.

6.1 ILE2T:RPM3

The first measurements performed were tests of the first Einzel lens, TIS1:EL1, using the Rotary Profile Monitor (ILE2T:RPM3) just downstream. The structure of TIS1:EL1 is shown in Figure 2, and the location of the RPM is shown in Figure 3. The RPM allows for an analysis of the location of the Einzel lens focal point as the lens bias is adjusted, provided all other elements are kept constant. Measurements were performed using ILE2T:RPM3 varying the value of TIS1:EL1 for 12keV, 15keV, and 20keV beam energies.

Measurements of the horizontal (x) and vertical (y) beam widths were taken and compared to the TRANSOPTR simulated beam envelope, which is cylindrically symmetric at ILE2T:RPM3. No emittance measurements were readily available for the simulation, however there is a 1cm aperture right after the TIS, so it was assumed that the initial beam was parallel and 1cm in radius due to collimation. Note that there are 2 sets of data points for measured values as the RPM scans beam once on the way in and once on the way out. An example of the raw data for 12keV beam energy with TIS1:EL1 set to 5200V can be found on Figure 20, and can be compared to the TRANSOPTR model in Figure 21. The measured width data for 12keV x and y can be found at Figure 22a and 22c, as compared to the TRANSOPTR width in Figure 22b.

These measurements were then repeated for 15keV and 20keV beam energies. An example of the raw data is given on Figures 23 and 26, and can again be compared to the TRANSOPTR model in Figures 24 and 27. Measured data can be found in Figures 25 and 28, with Figures (a) and (c) again being the measured horizontal and vertical widths while (b) is the TRANSOPTR simulated width.

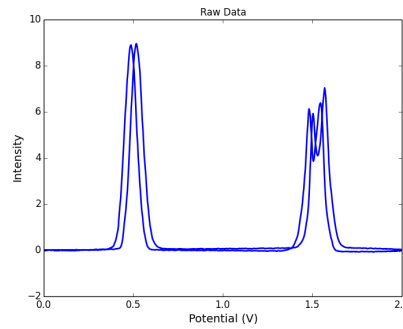


Figure 20: Raw RPM data at 12keV for TIS1:EL1 set to 5200V. The y-axis is an arbitrary intensity as measured by the RPM, while the x-axis is in inches.

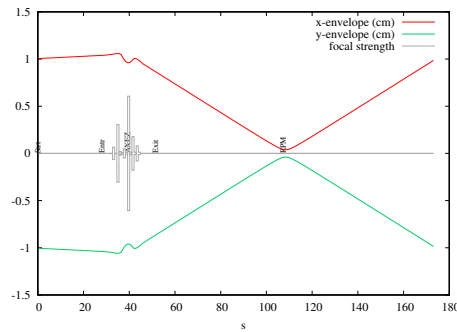


Figure 21: TRANSOPTR simulation of TIS beam line area at 12keV showing the location of the Einzel lens (set to 5200V) and the focus point at the RPM.

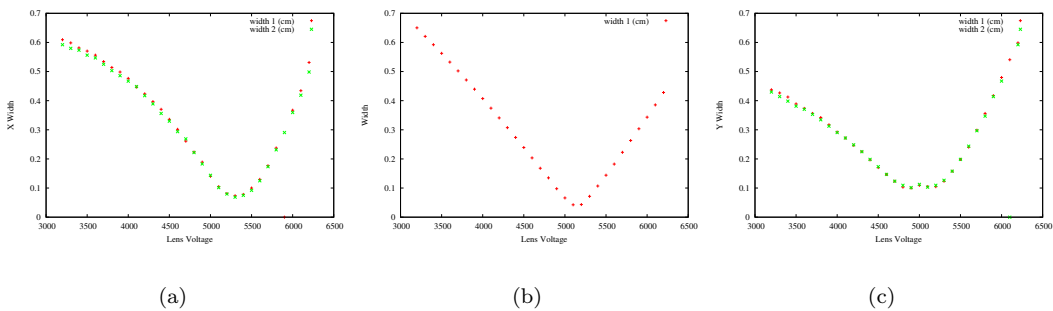


Figure 22: (a) Measured horizontal width of beam line at 12keV using both scans of ILE2T:RPM3 for a variety of TIS1:EL1 settings. (b) Simulated widths taken from TRANSOPTR at 12keV for a variety of TIS1:EL1 settings. (c) Measured vertical width of beam line at 12keV using both scans of ILE2T:RPM3 for a variety of TIS1:EL1 settings.

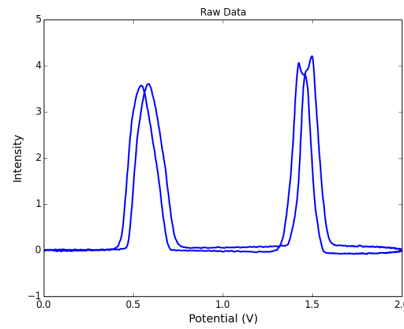


Figure 23: Raw RPM data at 15keV for TIS1:EL1 set to 6400V. The y-axis is an arbitrary intensity as measured by the RPM, while the x-axis is in inches.

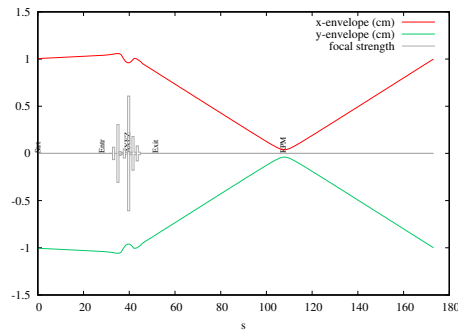


Figure 24: TRANSOPTR simulation of TIS beam line area at 15keV showing the location of the Einzel lens (set to 6400V) and the focus point at the RPM.

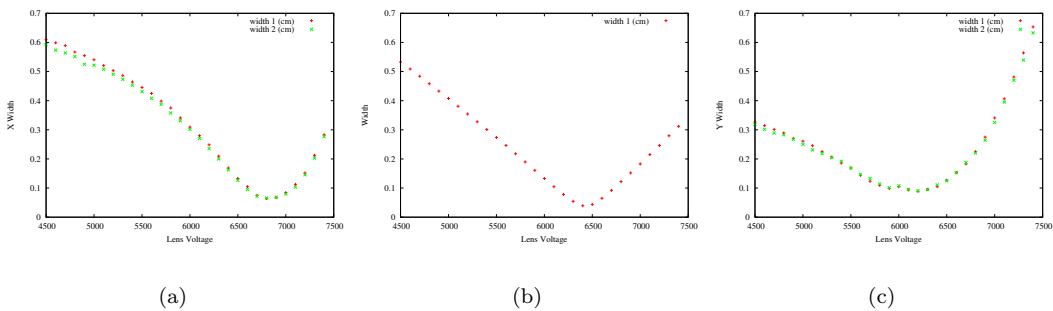


Figure 25: (a) Measured horizontal width of beam line at 15keV using both scans of ILE2T:RPM3 for a variety of TIS1:EL1 settings. (b) Simulated widths taken from TRANSOPTR at 15keV for a variety of TIS1:EL1 settings. (c) Measured vertical width of beam line at 15keV using both scans of ILE2T:RPM3 for a variety of TIS1:EL1 settings.

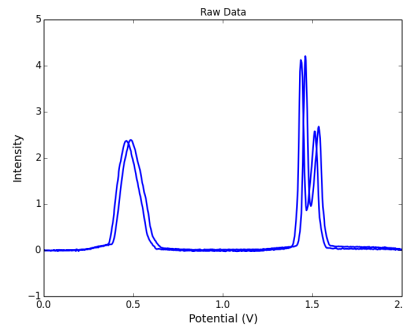


Figure 26: Raw RPM data at 20keV for TIS1:EL1 set to 8500V. The y-axis is an arbitrary intensity as measured by the RPM, while the x-axis is in inches.

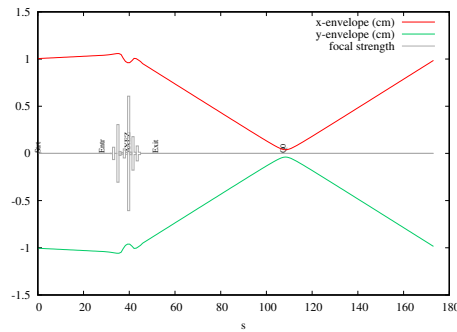


Figure 27: TRANSOPTR simulation of TIS beam line area at 20keV showing the location of the Einzel lens (set to 8500V) and the focus point at the RPM.

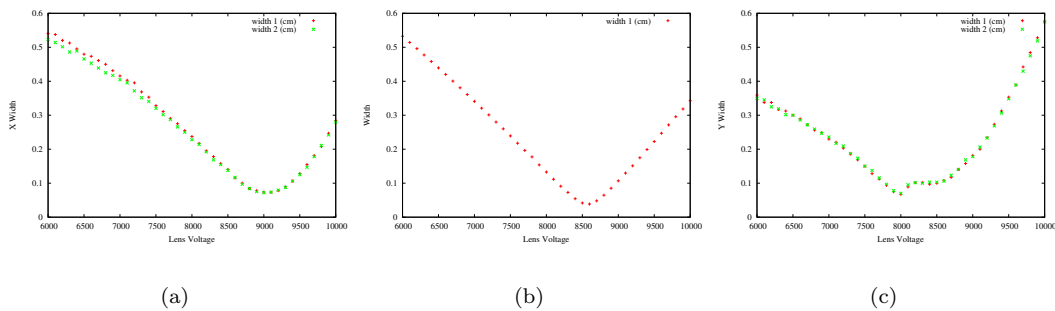


Figure 28: (a) Measured horizontal width of beam line at 20keV using both scans of ILE2T:RPM3 for a variety of TIS1:EL1 settings. (b) Simulated widths taken from TRANSOPTR at 20keV for a variety of TIS1:EL1 settings. (c) Measured vertical width of beam line at 20keV using both scans of ILE2T:RPM3 for a variety of TIS1:EL1 settings.

As shown in Figures 1 and 2, there is only one set of steering plates before entry into TIS1:EL1. Therefore the beam centroid cannot be displaced and as such the beam could not be made to follow a collinear trajectory along the central optical axis of the lens. This likely causes asymmetric focussing forces which introduce some steering effects within the Einzel lens. These forces cannot be accounted for in TRANSOPTR, which likely contributes to the horizontal and vertical measurements not perfectly agreeing with the model. Keeping this fact in mind, the horizontal and vertical centroid of the beam was also measured and recorded at 3 different energies, as shown in Figures 29, 30, and 31. Would the beam have been centred and collinear to the optical axis, we would not observe significant centroid shifts with varying lens voltage.

Again looking at Figures 1 and 2, there are multiple apertures that the beam must pass through before reaching the Einzel lens. The malformed peak that occurs at the focal point, as seen in Figures 20 and 26, could be due to the beam skimming one of these apertures, or an aperture closer to the RPM, or possibly from the source itself. It was not possible to positively determine the cause for this feature.

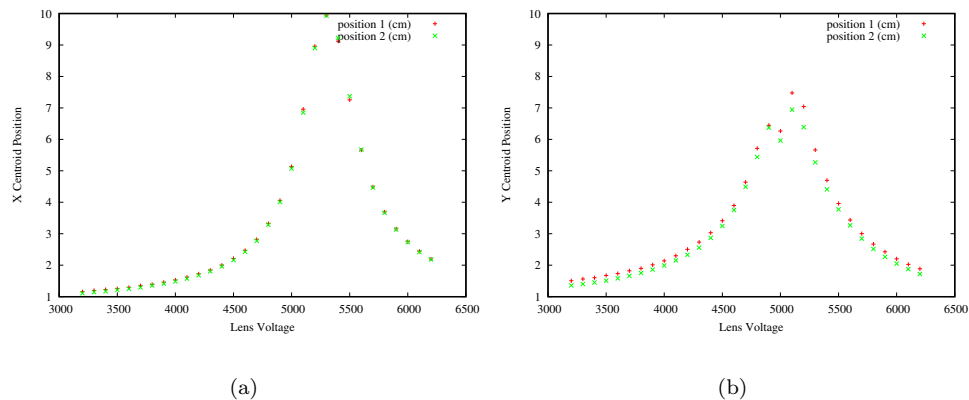


Figure 29: (a) Measured horizontal centroid position of beam at 12keV using both scans of ILE2T:RPM3 for a variety of TIS1:EL1 settings. (b) Measured vertical centroid position of beam at 12keV using both scans of ILE2T:RPM3 for a variety of TIS1:EL1 settings. Observe the "spike" feature.

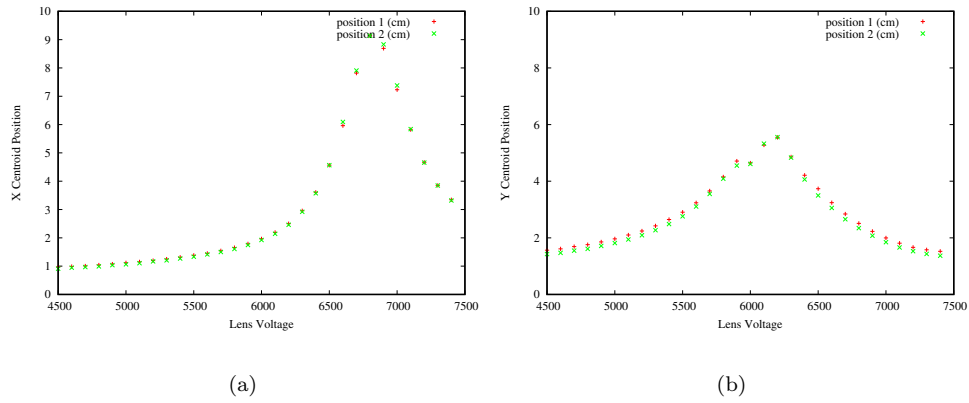


Figure 30: (a) Measured horizontal centroid position of beam at 15keV using both scans of ILE2T:RPM3 for a variety of TIS1:EL1 settings. (b) Measured vertical centroid position of beam at 15keV using both scans of ILE2T:RPM3 for a variety of TIS1:EL1 settings. Observe the "spike" feature.

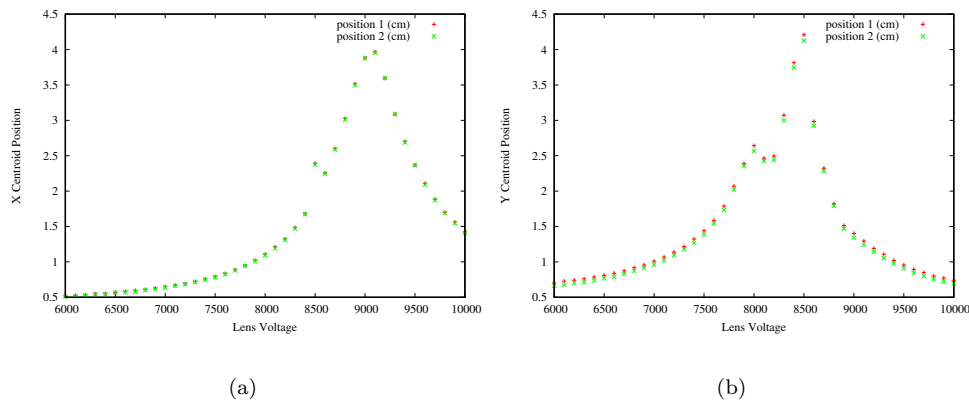


Figure 31: (a) Measured horizontal centroid position of beam at 20keV using both scans of ILE2T:RPM3 for a variety of TIS1:EL1 settings. (b) Measured vertical centroid position of beam at 20keV using both scans of ILE2T:RPM3 for a variety of TIS1:EL1 settings. Observe the "spike" feature.

Envelope behaviour as shown in Figures 22, 25, and 28, in addition to the strong centroid steering observed in Figures Figures 29, 30, and 31 support the inference that the Opera2D mappings produce a faithful simulation of the Einzel lens, and that the discrepancies are due to centroid offset effects. However, further testing in which this may be fully accounted for is required.

6.2 TRFCBL:MCP1

The next experiment conducted used the micro-channel plate (MCP) located in between the 45 degree bends, downstream of the RFQ. For reference, see Figure 3 or 4; TRFCBL:MCP1 sits in between TRFCBL:Q2 and TRFCBL:Q3, but was added to the beam line after these drawings were created and so is not shown explicitly. While the MCP has no quantitative digital imaging capabilities, TRFCBL:MCP1 contains a phosphorus screen and a view port, which allows sighting or external imaging of the beam spot on the MCP as seen in Figure 32.

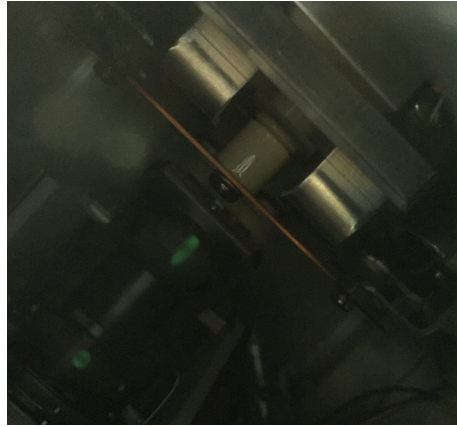


Figure 32: Example of photograph taken at TRFCBL:MCP1 at 5keV for TRFC:EL5 set to 3000V, showing beam pipe set up and beam spot on phosphorus screen. The beam spot is visible as a faint green spot, slightly below and left of the image centre.

The initial course of action for this test was to use a camera provided by the TITAN experiment to test the Opera2D model of TRFC:EL5 by taking images of the beam spot created by this phosphorus screen. However while a camera was provided, it proved impractical as the plug to connect to the computer was outdated. Instead, a mobile phone camera was used. While keeping the mobile phone steady was attempted, the lack of tripod or any stabilizing equipment inevitably lead to unaligned images. This meant that aligning the images needed to be completed in order for comparison between them to be accurate, which allowed for influences of human error.

All image processing, including alignment and the following measurements, was completed using the image manipulation program GIMP. To evaluate the horizontal and vertical width of the beam spot, a measurement tool in GIMP was used to provide the number of pixels defining the width of the imaged beam spot. A baseline image with a very skinny beam spot corresponding to a large envelope in one dimension and a skinny one in the other was chosen, and images were aligned by aligning the visible beam line features in the image, such as the plates next to the phosphorus screen. With this done, the aligned images were compared. This allowed for the extractions of relative envelope dimensions with respect to one another.

The horizontal envelope data from these measurements can be seen in Figures 33, 35 and 37, and the vertical envelopes in 34, 36 and 38 at 2keV, 5keV, and 10keV beam energies

respectively. Note that Figure (a) corresponds to the measured data from this image manipulation procedure, while Figure (b) corresponds to the matching TRANSOPTR prediction for the same TRFC:EL5 settings.

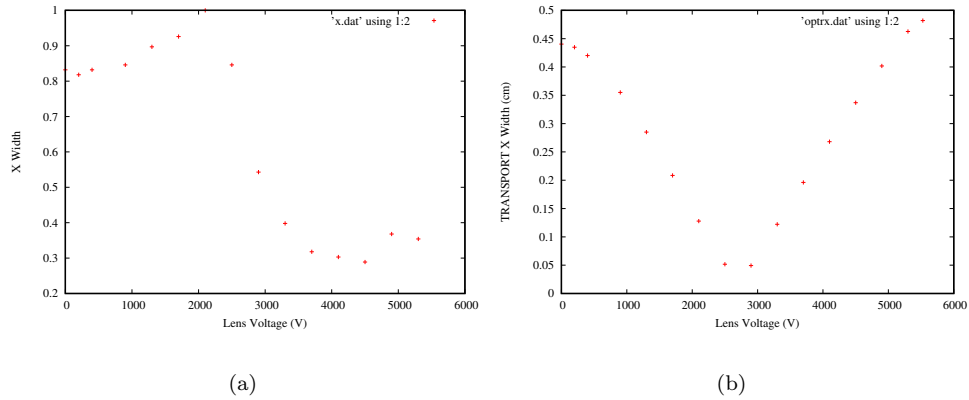


Figure 33: (a) Measured horizontal width of beam at 2keV for a variety of TIS1:EL1 settings. (b) TRANSOPTR calculated horizontal width of beam at 2keV for a variety of TIS1:EL1 settings.

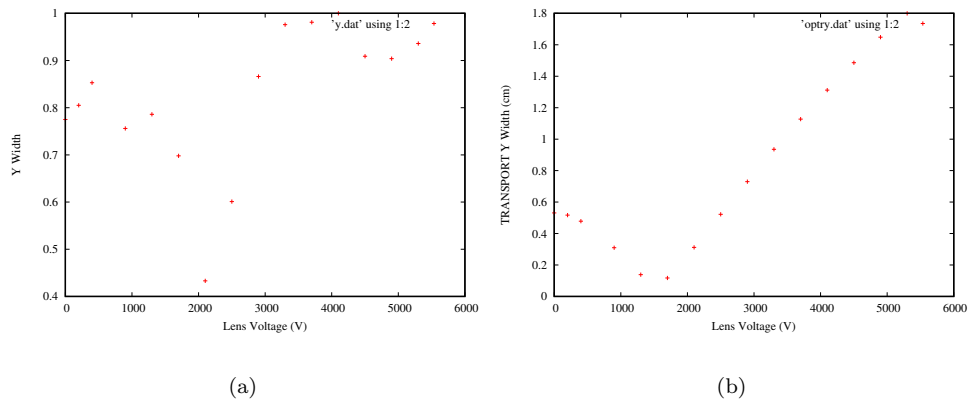


Figure 34: (a) Measured vertical width of beam at 2keV for a variety of TIS1:EL1 settings. (b) TRANSOPTR calculated vertical width of beam at 2keV for a variety of TIS1:EL1 settings.

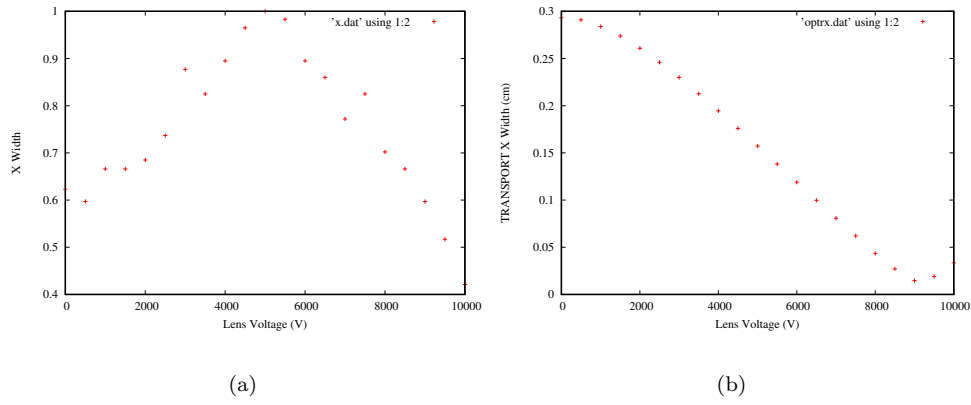


Figure 35: (a) Measured horizontal width of beam at 5keV for a variety of TIS1:EL1 settings. (b) TRANSPORT calculated horizontal width of beam at 5keV for a variety of TIS1:EL1 settings.

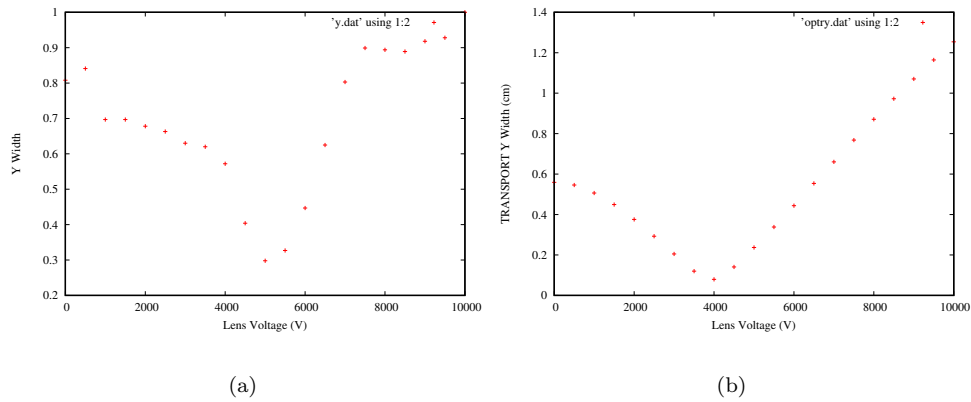


Figure 36: (a) Measured vertical width of beam at 5keV for a variety of TIS1:EL1 settings. (b) TRANSPORT calculated vertical width of beam at 5keV for a variety of TIS1:EL1 settings.

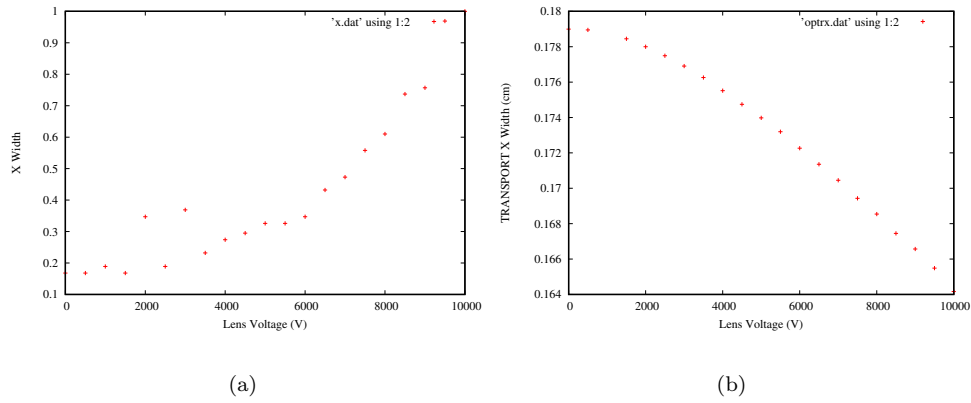


Figure 37: (a) Measured horizontal width of beam at 10keV for a variety of TIS1:EL1 settings. (b) TRANSOPTR calculated horizontal width of beam at 10keV for a variety of TIS1:EL1 settings.

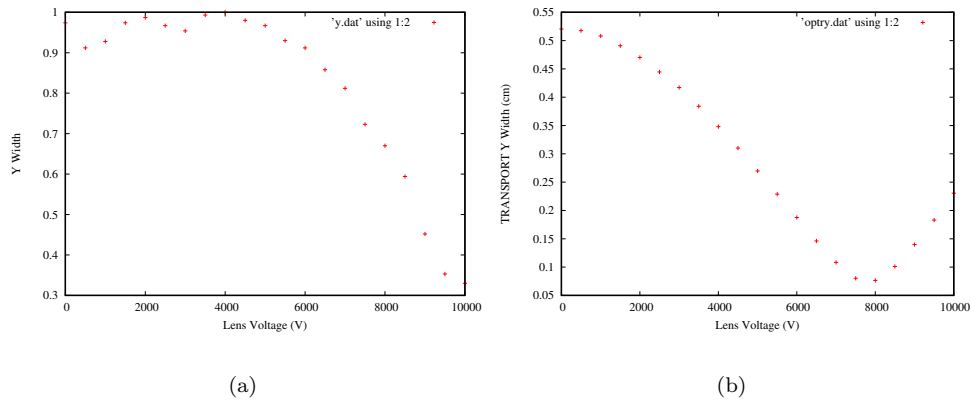


Figure 38: (a) Measured vertical width of beam at 10keV for a variety of TIS1:EL1 settings. (b) TRANSOPTR calculated vertical width of beam at 10keV for a variety of TIS1:EL1 settings.

When comparing the figures above, it is important to keep in mind that the widths measured are presented relative to each other, and not in centimetres like the TRANSOPTR calculations. Because of this unit discrepancy, the data can only be compared as trends and not points. If these measurements were to be repeated, a suggested change to the procedure would be to include a 1cm piece of tape as a conversion factor on the view point. This way when measuring the width in pixels of the beam spot, not only is it simple to convert pixels to centimetres, but there is also an indicator as to whether or not the images are aligned.

While these measurements, particularly the y-envelope comparisons in Figures 34, 36, and 38, tend to support the Opera2D model of TRFC:EL5 the margin of error in the experiment was too large to fully conclude anything definite. The quantitative data that would be provided from a fixed diagnostic element in that position (such as an RPM) would be more valuable in determining the beam size and tracking its changes than the current diagnostic set up. It would also allow for more robust tuning of beam centroids, aiming to minimized unwanted steering effects due to misalignment. Along the TSYBL beam line shown in Figure 4 there are multiple Einzel lenses that were modelled in Opera2D whose potential maps were not tested for accuracy. This was due to a lack of diagnostic elements that could provide beam size data along that beam line and to MPET.

It is also very likely that the discrepancies are in part due to the beam centroid offsets in the 90° bend, causing additional steering by the quadrupoles. Indeed, it was observed that using the available phosphorus MCP in the 90° bend rendered the setup of good beam alignment through the section difficult. In effect, the degree of centring can at present only be inferred, for example by the asymmetries in the envelope shape on the MCP, as shown in Figures 33, 34, 35, 36, 37, and 38.

The inability to directly observe the beam envelope in a diagnostic read back at the 90° bend causes the tuning of RFQ extracted beam extremely difficult, particularly when considering the aperture constraints present in the horizontal beam line segment to MPET, which includes a 4mm wide and 12cm long differential pumping aperture. As a result, the present report strongly recommends the exploration of additional beam line diagnostics for the TITAN experiment. Not only would this enable easier and more robust testing of the TITAN beam line simulations, including the Opera2D modelled elements, but it would likely considerably shorten tuning times and enable further development of HLA's for the TITAN experiment.

7 Conclusion

The present report spans the progress of implementing the TITAN Optics system into the HLA framework. This began with taking measurements on design drawings provided by the TRIUMF design office to determine the positions and attributes of the elements along the TITAN transport beam line to MPET. These positions were then recorded in the `/acc` database where they can be used by HLA's as well as run in `TRANSOPTR` through a Python script `xml2optr`. However, the field maps from the Einzel lenses present along the beam line could not be accurately reproduced using the generic `TRANSOPTR` subroutine, so they were modelled using Opera2D. Once the Einzel lens potential maps were included in the `/acc` database, `TRANSOPTR` simulations could be run to calculate the beam envelope through the TITAN beam line.

Measurements using the TIS were performed to test the Opera2D models of the lenses, as well as the accurate positions of the elements from the drawings. Using ILE2T:RPM3 and varying TIS1:EL1, measured beam widths were compared to `TRANSOPTR` calculations, and centroid variations were also recorded. Measurements were also taken using the phosphorus screen on TRFCBL:MCP1 by taking photos of the beam spot through the view port while varying TRFC:EL5, and using image processing later to extract the relative widths to again compared to `TRANSOPTR` calculated widths.

While the above measurements lend credence to the Opera2D models, the present diagnostic configuration in the TITAN system, particularly in the 90° bend following the RFQ, rendered precise data acquisition difficult. As such, further testing is needed to fully validate the accuracy of the potential maps. The discrepancies present could be due to the offsets of the beam centroid causing additional steering effects in the optical elements such as Einzel lenses and quadrupoles. The present diagnostic elements are not sufficient to draw strong conclusions. The continuation of this testing likely would shorten time taken to tune beam through TITAN transport beam line, in addition to allowing more efficient troubleshooting. Further, it would enable further development of the HLA's serving the TITAN experiment.

References

- [1] P Delheij, L Blomeley, M Froese, G Gwinner, V Ryjov, M Smith, and J Dilling. *The TITAN mass measurement facility at TRIUMF-ISAC*. In *TCP 2006*, pages 279–287. Springer, 2007.
- [2] Carla Barquest, Margaret Corwin, Paul Jung, Spencer Kiy, Kevin Lucow, Samantha Marcano, Thomas Planche, Stephanie Rädcl, Brad Schultz, Dan Sehayek, et al. *Web-Based Control Room Applications at TRIUMF*. In *9th Int. Particle Accelerator Conf. (IPAC'18), Vancouver, BC, Canada, April 29-May 4, 2018*, pages 4832–4835. JACOW Publishing, Geneva, Switzerland, 2018.
- [3] EA Heighway and Mark Sybe De Jong. *TRANSOPTR—a beam transport design code with space charge, automatic internal optimization and general constraints*. Technical report, CM-P00068120, 1984.
- [4] R Baartman. *TRANSOPTR: Changes since 1984*. TRIUMF, Vancouver, Canada, Rep. TRI-BN-16-06, 2016.
- [5] Vector Fields. *Opera-2d user guide*. Vector Fields Limited, England, 1999.
- [6] Dassault Systemes. *DraftSight: Professional-grade, free* CAD software*, 2012.